symmetry

IMPACT FACTOR 2.7

CITESCORE 4.9

Review

Review of Flavor Anomalies

Seema Bahinipati

Special Issue

Symmetry in Hadron and Quark Models

Edited by

Dr. Sergey Mikhailovich Polikarpov

MDPI

https://doi.org/10.3390/sym15101963

symmetry

MDPI

Review

Review of Flavor Anomalies

Seema Bahinipati

School of Basic Sciences, Indian Institute of Technology Bhubaneswar, Bhubaneswar 752050, Odisha, India; seema.bahinipati@iitbbs.ac.in

Abstract: Lepton flavor universality exists in the Standard Model, and hence any observation of the violation of this universality will be a hint for new physics. Recent experimental searches for processes violating this symmetry have attracted much attention among theorists and experimentalists alike. In recent years, such hints have been observed in flavor changing neutral current weak processes such as $b \to sll$ and charged current weak processes such as $b \to cl\nu$ processes by collider experiments like Belle, Belle II, BaBar, LHCb, ATLAS, and CMS collaborations, where b, s, c are the bottom, strange, and charm quarks, respectively, and l, ν stand for lepton and the corresponding lepton neutrino, respectively. This article is a review of some of the interesting anomalies observed in the B-sector and includes decays of B_s mesons.

Keywords: lepton flavor universality; new physics; colliders

check for updates

Citation: Bahinipati, S. Review of Flavor Anomalies. *Symmetry* **2023**, *15*, 1963. https://doi.org/10.3390/sym15101963

Academic Editors: Gui Jun Ding and Janusz Gluza

Received: 21 April 2023
Revised: 2 October 2023
Accepted: 10 October 2023
Published: 23 October 2023

1. Introduction

The fundamental fermions of the Standard Model (SM), quarks and leptons, exist in three generations, each of which consists of two members. By the lepton flavor universality (LFU) symmetry, we mean that the coupling strength of the electroweak gauge bosons to the three families of leptons is the same. The only exception to this concept of universality can be attributed to the Higgs field, since the lepton–Higgs interaction strength leads to a difference in the lepton masses and a specific mass hierarchy of $m_e < m_\mu < m_\tau$. Hence, any signature of violation of this symmetry would mean a deviation from the SM, which is called new physics (NP) [1]. Evidence of NP would imply either new particles or new phenomena that have not been observed yet.

Although the SM is mostly a well-tested theory in particle physics, there are still several flavor puzzles that are unsolved: why there are only three generations of fundamental particles, what is the origin of the mass hierarchy in quarks and leptons, and why is the quark flavor mixing matrix hierarchical and nearly diagonal. To probe these mysteries, two approaches can be used: a direct one or an indirect one.

The observed differences in the coupling strengths in the nuclear β-decays, muon decays, pion decays, and kaon decays have led to the belief that either the weak interaction coupling constant is not universal or there is something else going on. These observations, such as the approximately 20 times slower decay rate for $K^- \to \mu^- \bar{\nu_\mu}$ compared to the $\pi^- \to \mu^- \bar{\nu_\mu}$, were explained by the Cabibbo hypothesis [2]. This profound hypothesis proposed by Cabibbo stated that the weak interaction eigenstates are not the same as the mass eigenstates and paved the way towards the need for a fourth quark, named the "charm" quark.

However, when the Cabibbo hypothesis was first proposed, the charm quark had not been discovered yet. The Cabibbo hypothesis could nicely explain the differences observed in several weak decays, but was unable to explain why the observed branching ratio was smaller than expected for the flavor-changing neutral current process, $K_L \to \mu^+\mu^-$. It was only in 1970, when Glashow, Iliopoulos, and Maiani (GIM) predicted the existence of the fourth ("charm") quark, that the $K_L \to \mu^+\mu^-$ could proceed via the exchange of a virtual charm quark in addition to the exchange of a virtual up-quark, thus explaining the

suppression of the decay rate for the process. This mechanism, called the GIM mechanism, can be considered one of the first important chapters in the story of flavor anomalies.

The understanding of the suppression of $b \to s$ transitions is grounded in the fundamental symmetries upon which the SM is constructed. Nevertheless, it is important to note that lepton universality is not an inherent property derived from any fundamental principle or axiom within the SM. There exist theoretical extensions to the SM that propose the existence of additional virtual particles, such as lepto-quarks. These particles could potentially play a role in $b \to s$ transitions, as depicted in Figure 1 (right). Furthermore, these extensions suggest that these particles may exhibit non-universal interactions, leading to discrepancies between the observed branching fractions of $B^+ \to K^+ l^+ l^-$ decays and the predictions made by the SM.

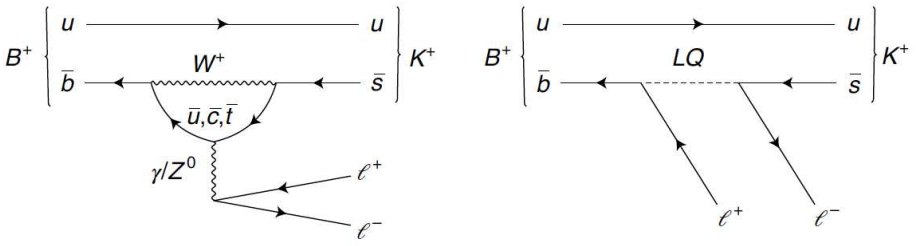

Figure 1. Main Feynman diagrams contributing to the $B^+ \to K^+ ll$ decay in SM (**left**) and possible contributions from extensions to SM (**right**).

Quantum chromodynamics (QCD) calculations dominate the theoretical predictions for the branching fractions of $b \to sll$ processes, $B^+ \to K^+\mu^+\mu^-$ and $B^+ \to K^+e^+e^-$ decays, and this makes these predictions complicated. The large coupling constant of strong interactions makes these predictions difficult, as it is hard to compute the electroweak amplitudes using perturbation techniques. Only approximate calculations can be made. However, since leptons do not carry a "color" charge, the strong force does not couple directly to leptons. This is advantageous for the $b \to sll$ processes, and as a result, the ratio of the branching fractions of the $B^+ \to K^+\mu^+\mu^-$ and $B^+ \to K^+e^+e^-$ decays may be predicted with an accuracy of $O(1\%)$. The anticipated ratio is expected to approximate unity due to the relatively smaller masses of electrons and muons compared to those of bottom quarks. Typically, this scenario holds true, unless the magnitude of the dilepton invariant mass-squared (q^2) imposes substantial limitations on the phase space that may accommodate the formation of the two leptons. The same line of reasoning may be applied to decays involving various B hadrons, $B \to X\mu^+\mu^-$, and $B \to Xe^+e^-$, where $B = B^+, B^0, B_s^0$ mesons, or Λ_b^0 baryons. In these decays, X can refer to an excited kaon, K^{*0}, or a composite particle such as a proton and charged kaon (pK).

2. Major Experimental Facilities

The primary experiments that have made significant contributions to the investigation of b-hadron decays associated with flavor anomalies include the B-factory experiments BaBar [3] and Belle [4], the Tevatron experiments CDF [5] and DØ [6], and the Large Hadron Collider (LHC) experiments ATLAS [7], CMS [8], and LHCb [9]. One notable advantage of the Belle II and BaBar detectors is their pristine working environment, which may be attributed to their use in e^+–e^- colliders. In contrast, the CMS, ATLAS, and LHCb detectors face the challenge of functioning in a more hostile environment due to their involvement in hadron collisions at the LHC.

3. Flavor Anomalies in the B-Sector

The decays used to study LFU are extremely rare, as such processes involve cross-generational couplings, such as $b \to s$, which is a Cabibbo-suppressed process in the SM (Figure 2). LFU can be affected if there is the presence of new particles or new processes.

Searches for such particles are performed at the LHC. However, these particles are still undiscovered, since higher energies are needed to detect these unknown particles.

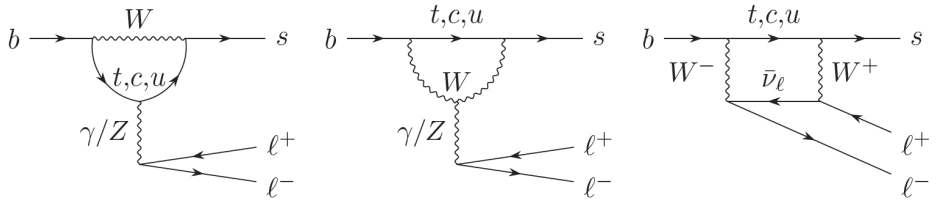

Figure 2. Loop-level Feynman diagrams for $b \to sll$ decays.

For the cross-generational $b \to s$ transitions, LFU is tested by comparing the ratios of decay rates of beauty particles into different leptons. Recent results had caused a stir due to the observation of some hints of deviation in LFU, but they were not statistically significant enough. Hence, until now, we have not concluded emphatically that LFU in the SM is violated. In any case, the observed deviations from the predictions have opened the doors for the possibility of the existence of physics beyond the SM.

3.1. R_K, R_{K^*} Analyses

Understanding the decay of b-hadrons is challenging since these decays can be studied at several different energy scales, such as electro-weak, natural, and hadronic scales. One can use effective field theories (EFTs) to disentangle these scales and thus provide predictions for these b-decays with greater accuracy. Wilson coefficients are key ingredients in the weak effective field theory that contain the effects of SM fields. These coefficients provide information about the SM and beyond-SM contributions. The rare *b*-decays can be explained using Hamiltonians involving the Wilson coefficients in a framework called operator product expansion (OPE) [10], a model-independent analysis of effects beyond the SM. In particular, $b \to sll$ transitions are described by the effective Hamiltonian:

$$\mathcal{H}_{eff} = -4(G_F/\sqrt{2})V_{tb}V_{ts}^* \sum_{i=1}^{12} (\mathcal{C}_i \mathcal{O}_i + \mathcal{C}'_i \mathcal{O}'_i).$$

Here, G_F is the Fermi coupling constant, V_{ij} are the elements of the Cabibbo–Kobayashi–Maskawa (CKM) matrix [11], $O_i^{'}$ are the local operators containing left(right)-handed long distance contributions, and $C_i^{'}$ are the corresponding Wilson coefficients. Here, O_7 is the electromagnetic operator and O_9 and O_{10} are the semileptonic operators, and their chirally flipped counterparts are $O_7^{'}$, $O_9^{'}$, and $O_{10}^{'}$.

The experimental observations show disagreement with the SM predictions in decays dominated by the effective vector and axial-vector couplings $\mathcal{C}_9$ and $\mathcal{C}_{10}$. The SM expectations exceed the observed value for these decays. In these cases, a SM explanation is possible for the statistical significance of these results. Still, there are several variables wherein the tension still exists or the verdict of the agreement with SM can change with the accumulation of more data. Thus, it is difficult to make a conclusive statement now.

In the $b \to sll$, $l = e, \mu$ analyses, the observable that is determined is R_h, where $h = K^{(*)}$, defined as follows:

$$R_h = \frac{\Gamma(B \to h\mu\mu)}{\Gamma(B \to hee)}$$

The SM predicts this ratio to be unity, as there is no preferential coupling of the gauge-bosons to leptons of any generation. The advantage in determining R_h, where $h = K^{(*)}$, is that the hadronic uncertainties mostly cancel out in the SM for this ratio, assuming the momentum transfer to the lepton pair is sufficiently large. These observables are predicted to have unity with uncertainties below 1%. There are several experiments, such as Belle, LHCb, and other experiments [12–18], and Refs. [19–24] have performed these LFU tests.

The observables are specified as ratios of yields that have been corrected for efficiency within a specific range of di-lepton invariant squared (q^2) values. This range excludes the resonant channels that involve the J/ψ and $\psi(2S)$ resonances. The present analyses utilize decay modes that involve J/ψ and $\psi(2S)$ as control channels. Control channels are selected based on their larger branching percentage and well-measured nature, with the mode containing J/ψ being particularly favored. As an example, the decay processes $B_s \to \phi ll$, $B_s \to J/\psi\phi$ are employed as control modes. Due to the similarity of the final state particles in both the uncommon and resonant decay modes, a number of systematic uncertainties cancel out.

The angular distribution of particles generated in $B^{*0} \to K^{*0}\mu^+\mu^-$ decays was analysed by LHCb. This analysis utilized data from the Run 1 data [25] and involved the measurement of angular parameters, namely the charge-conjugation parity (CP)-averaged observable $P_5^{'}$. The measurement was conducted using an unbinned maximum likelihood fit. The measurement is conducted within specific ranges of dimuon invariant mass squared (q^2) to deliberately remove charmonium resonances J/ψ and $\psi(2S)$. The majority of observables exhibit a high level of concordance with the Standard Model. Nevertheless, a noteworthy level of stress (3.4 σ) [25] is detected in $P_5^{'}$. Other studies, like ATLAS [12] and Belle [14], have also observed a similar tension between theory and experiment, albeit with greater uncertainty. The study conducted by CMS [13] demonstrates agreement with the Standard Model (SM), while also being consistent with other experimental observations. The angular observable $P_5^{'}$ in $B^{*0} \to K^{*0}\mu^+\mu^-$ decays in the bins dimuon invariant mass squared $(q^2)\epsilon[4.0, 6.0]$, $[4.3, 6.0]$ and $[4.0, 8.0]$ from ATLAS [12], LHCb [26,27], CMS [13], and Belle [14] deviate at 3.3 σ, 1 σ, and 2.1 σ from the SM expectations [28,29], respectively.

The first simultaneous test of muon-electron universality was performed by LHCb in proton–proton collisions collected with the LHCb detector between 2011 and 2018 [30,31]. The LFU tests are performed as a double ratio, $R_{(K,K^{(*)})}$.

$$R_{(K,K^{(*)})} = \frac{N/\epsilon(B^{+,*0} \to K^{+,*0}\mu^+\mu^-)}{N/\epsilon(B^{+,*0} \to J/\psi^{+,*0}\mu^+\mu^-)} / \frac{N/\epsilon(B^{+,*0} \to K^{+,*0}e^+e^-)}{N/\epsilon(B^{+,*0} \to J/\psi^{+,*0}e^+e^-)}$$

$N/\epsilon(X)$ stands for the efficiency-corrected resonant mode yields. The $R_{(K,K^{(*)})}$ is measured in two q^2 intervals: $0.1 < q^2 < 1.1\ GeV^2$, referred to as low-q^2, and $1.1 < q^2 < 6.0\ GeV^2$, referred to as central-q^2.

Four efficiency-corrected resonant mode yield ratios are defined as benchmarks for this analysis. The double ratio is evaluated using a simultaneous maximum-likelihood fit to the B^+ and B^0 candidate invariant masses in the low-q^2 and central-q^2 regions (Figure 3), where the efficiencies are constrained using values and uncertainties obtained from simulated data. These results are in agreement with the SM predictions.

The latest LHCb results presented differ from their previous measurements of R_K and R_{K^*}, which they supersede. The R_{K^*} analysis uses five times more B meson decays than the previous result. The latest measurement benefits from the use of tighter electron identification criteria and better modeling of the residual misidentified hadronic backgrounds. However, the statistical fluctuations make a smaller contribution to the difference since the same data are used as in the previous publication. Since the dominant uncertainty is statistical, inclusion of more data will help to improve the precision.

The previous LHCb R_K, $R_{K^{*+}}$ [19] result that used Run 1 data (center-of-mass energy, $\sqrt{s} = 7, 8\ TeV$) had a 2.5 σ deviation from the SM expectations, whereas the recent results [24] that included Run 2 data ($\sqrt{s} = 13\ TeV$) and are compatible with the SM within 0.2 σ. The measurement is still statistically dominant. The major source of systematic uncertainty is due to the estimation of the misidentified backgrounds using the data-driven method. In the latter result, the single misidentification, $\pi \to e$ or $K \to e$, amounted to a reduction of a factor of 1(2) in the $K \to e$ misidentification and that of 2(7) in the $K \to e$ misidentification in Run 1 (Run 2) results. In cases of double misidentification, this factor was further reduced. Thus, the new LHCb result yielded a smaller systematic

uncertainty and is the most precise result of LFU to date. The tension that arose from the deviation of 2.6 σ from the SM prediction appears to have dissipated. Nevertheless, the forthcoming outcomes using Run III data at higher center-of-mass energy may present novel and unexpected findings.

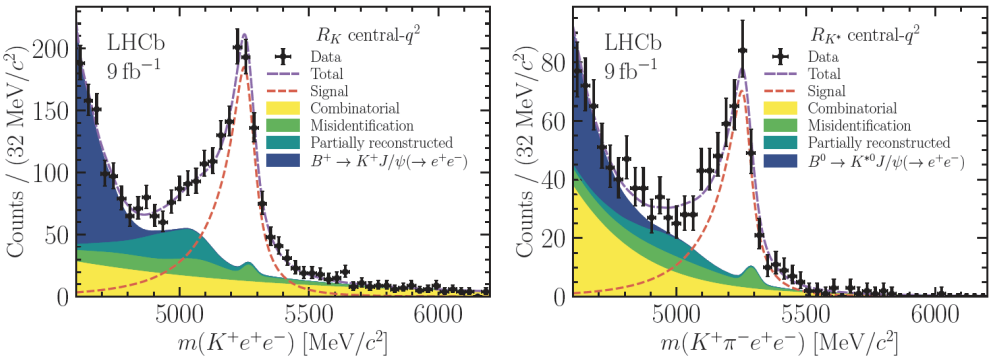

Figure 3. Invariant mass distributions of $B^+ \to K^+e^+e^-$ (**left**) and $B^+ \to K^+ {}^- e^+e^-$ (**right**) in the central-q^2 [31].

The $R(K^*)$ measurements at Belle II [32] are performed using the decay modes $B^0 \to K^{*0}(K^{+-})ll$ and $B^+ \to K^{*+}(K^{+0}, K_s^{0+})ll$. The background from continuum and generic $B\bar{B}$ decays is suppressed using a multivariate technique called a boosted decision tree (BDT), which includes event shapes, vertex quality, and kinematic variables. A two-dimensional unbinned maximum likelihood (UML) fit in the beam-energy-constrained mass $M_{bc} = \sqrt{{E^*_{beam}}^2 - {p^*_B}^2}$ and energy difference $\Delta E = E^*_B - E^*_{beam}$ variables. Here, E^*_{beam} is the beam energy. In the $e^+ - e^-$ center-of-mass frame, the momentum and energy of the B meson are represented by p^*_B and E^*_B, respectively.

Here, E^*_{beam} is the beam energy and p^*_B and E^*_B are the momentum and energy of the B meson in the $e^+ - e^-$ center-of-mass frame. The measurement of branching fractions encompasses the complete spectrum of dilepton mass, with the exception of the low mass range in order to minimize the interference from the $B \to K^*\gamma$ background and regions that are consistent with decays of the charmonium resonances. The findings align with global averages, accounting for the associated uncertainties.

Figures 4–6 provide a summary of R_K, $R_{K^{*+}}$ and $R_{K_s^0}$ from various experiments such as Belle [15–17], BaBar [18], LHCb [19–24]. The summary of results with the inclusion of the recent $R(K)$ result from LHCb is shown in Figure 5.

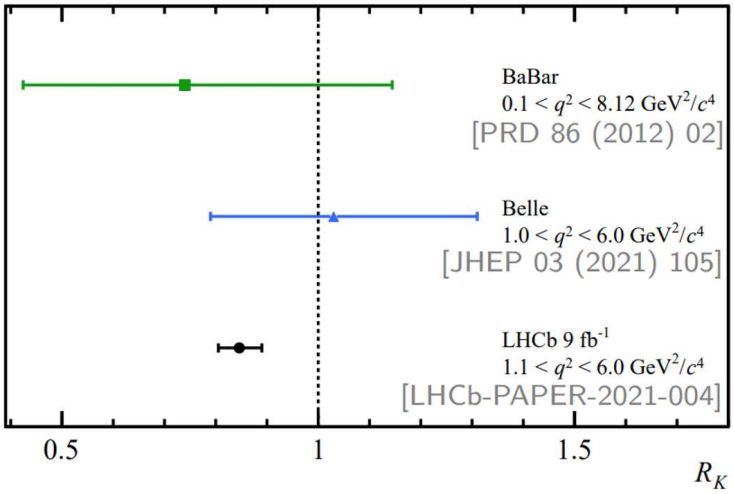

Figure 4. R_K for different q^2 regions by Belle, BaBar, and LHCb collaborations before the inclusion of the latest LHCb result.

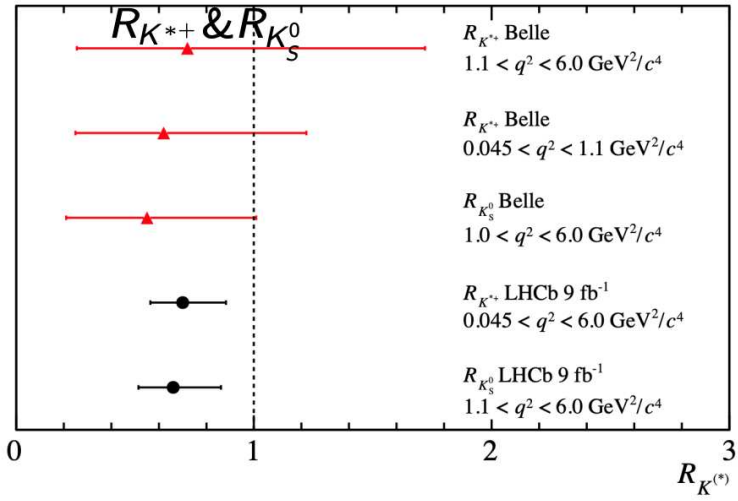

Figure 5. $R_{K^{*+}}$ and $R_{K^0_S}$ for different q^2 regions by Belle, BaBar, and LHCb collaborations.

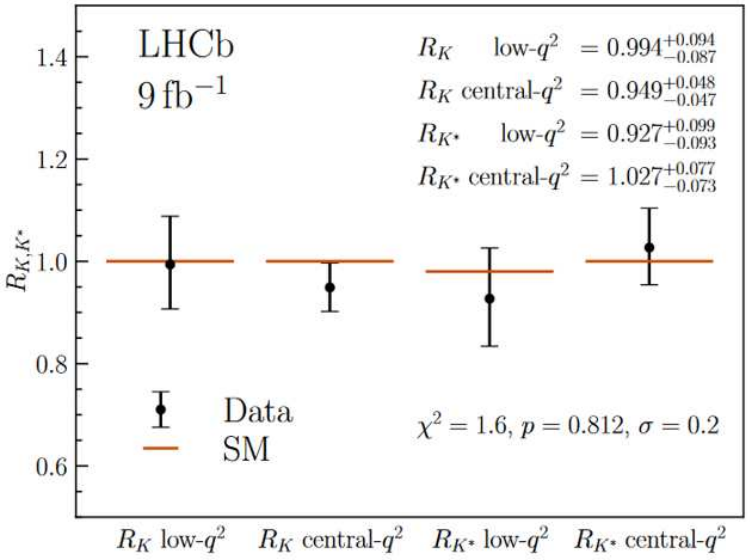

Figure 6. $R_{K^{(*)}}$ for low and central q^2 regions using 9 fb^{-1} data by LHCb collaboration.

3.2. $B_s \to \mu\mu$ Analyses

In the family of $b \to sll$ decays, there are the interesting decays of $B^0_s \to \mu^+\mu^-$ and $B^0 \to \mu^+\mu^-$. These decays have no tree-level contribution; rather, they can only occur via loop diagrams (Figure 7); thus, the expected branching fraction should be small. Further, these decays are also helicity suppressed, making them yet rarer. In the SM, the expected branching fractions of decay time-integrated branching fractions $B^0_s \to \mu^+\mu^-$ and $B^0 \to \mu^+\mu^-$ are $(3.66 \pm 0.14) \times 10^{-9}$ and $(1.03 \pm 0.05) \times 10^{-10}$, respectively. In recent years, significant advancements have been made in reducing the theoretical uncertainties associated with calculating branching fractions. These advancements can be attributed to progress made in lattice quantum chromodynamics (LQCD) [33,34], in the calculation of electroweak effects at next-to-leading order [35], and in the calculation of QCD effects at next-to-next-to-leading order [36].

CMS collaboration measured the time-integrated branching fraction of the $B(B^0_s \to \mu^+\mu^-)$ decays using both Run 1 and Run 2 data collected in pp collisions at the Large Hadron Collider (LHC) at CERN. The data correspond to integrated luminosities of 5 and 20 fb^{-1} recorded in the years 2011 and 2012 by the CMS detector at $\sqrt{s} = 7$ and 8 TeV, respectively, during the Run 1 data-taking period, and 36 fb^{-1} recorded in 2016 at $\sqrt{(s)}$ = 13 TeV during Run 2 data-taking period. $B^0_s \to \mu^+\mu^-$ decay is observed with

a significance of 5.6 standard deviations, and the branching fraction is measured as $B(B_s^0 \to \mu^+\mu^-) = [2.9 \pm 0.6(stat) \pm 0.3(syst) \pm 0.2(frag)] \times 10^{-9}$, where the last uncertainty refers to the uncertainty in the ratio of the B_s^0 and the B^+ fragmentation functions [37]. The highlights of this analysis were the usage of multi-variate techniques both for muon identification and candidate selection. The number of reconstructed events for the decays is obtained from the fits, and the efficiencies are used to obtain the branching fraction of the decay. The probability density functions (PDFs) obtained from simulated event samples, and data sidebands are used to perform the extended UML fit in the data (Figure 8).

As no significant observation of the $B^0 \to \mu^+\mu^-$ is observed, an upper limit $B(B^0 \to \mu^+\mu^-) < 3.6 \times 10^{-10}$ is determined at a 95% confidence level.

CMS also performed studies for the determination of the $B_s^0 \to \mu^+\mu^-$ effective lifetime. For this measurement, two independent procedures are used, namely a two-dimensional UML fit to the invariant mass (Figure 9) and proper decay time distributions of $B_s^0 \to \mu^+\mu^-$ candidates, and a one-dimensional (1D) binned maximum likelihood (ML) fit to the background-subtracted proper decay time distribution obtained with the sPlot [38] method. The $B_s^0 \to \mu^+\mu^-$ effective lifetime is found to be $[1.70 + 0.60 - 0.43(stat) \pm 0.09(syst)]$ ps. The measurement of the branching fractions [39] in this analysis supersedes the previous results from CMS. The observed branching fractions agree with the SM predictions.

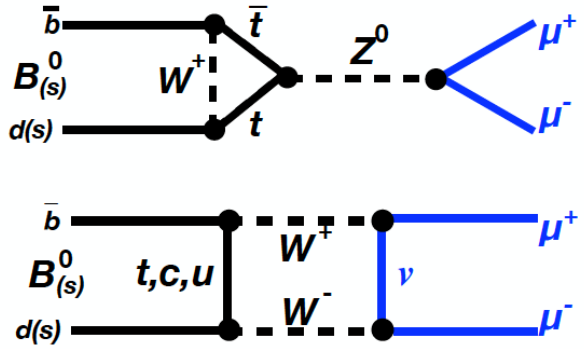

Figure 7. Loop-level diagrams for $B_s^0 \to \mu^+\mu^-$ decays.

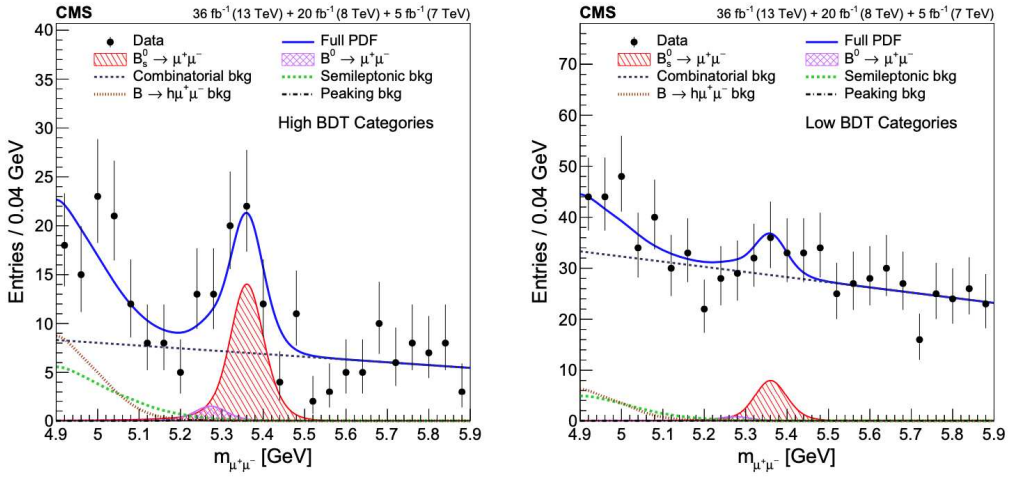

Figure 8. Invariant mass distributions with the fit projection. The left (right) plot shows the combined results from the high- (low-)range analysis boosted decision tree (BDT) selection categories [37]. The total fit is shown by the solid line, and the different background components are shown by the broken lines. The signal components are shown by the hatched distributions.

The branching fraction measurement of $B_s^0 \to \mu^+\mu^-$ and the B_s^0 effective lifetime, as well as the results of a search for the $B^0 \to \mu^+\mu^-$ decay, were performed using proton–proton collisions at $\sqrt{(s)} = 13$ TeV at the LHC [38]. The analysis is based on data collected

with the CMS detector in 2016–2018 corresponding to an integrated luminosity of 140 fb^{-1}. The branching fraction of the $B_s^0 \to \mu^+\mu^-$ decay and the effective B_s^0 meson lifetime are the most precise single measurements to date. No evidence for the $B^0 \to \mu^+\mu^-$ decay has been found. No deviation is observed with the SM predictions and previous measurements (Figure 9).

LHCb collaboration measured $B(B_s^0 \to \mu^+\mu^-) = (3.09^{+0.46}_{-0.43}(stat)^{+0.15}_{-0.11}(syst)) \times 10^{-9}$ [40], and the CMS collaboration measured $B(B_s^0 \to \mu^+\mu^-) = (3.83^{+0.38}_{-0.36}(stat)^{+0.24}_{-0.21}(syst)) \times 10^{-9}$ is about 1.2 standard deviations higher. The combination of both of these results brings the $B(B_s^0 \to \mu^+\mu^-)$ to be consistent with the SM prediction. So, the discrepancy between theoretical prediction and observation has been reduced.

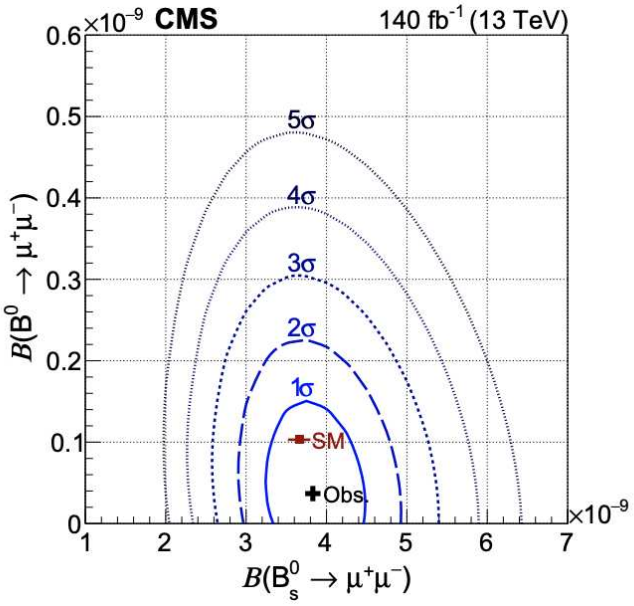

Figure 9. Profile likelihood [41] as a function of the branching fraction of $B_s^0 \to \mu^+\mu^-$ decay [39]. Contours in 2D enclose the regions with $1-5\,\sigma$ coverage, where 1, 2, and 3 σ regions correspond to 68.3, 95.4, and 99.7% confidence levels, respectively.

3.3. Inclusive $R(X_{e/\mu})$ Analysis

The first measurement of the inclusive branching fraction ratio $R(X_{e/\mu}) = B(B \to Xev/)/B(B \to X\mu\nu)$ was published by the Belle II collaboration. This measurement represents the most precise test of electron–muon universality in semileptonic B-meson decays up to the present time [42]. The Belle II collision data set was obtained during the period from 2019 to 2021, with a center-of-mass energy of $\sqrt{s} = 10.58\ GeV$. This energy level corresponds to the mass of the $\Upsilon(4S)$ resonance, which predominantly undergoes decay into a pair of B mesons of opposite flavor. The integrated luminosity of the data set is 189 fb^{-1}, equivalent to approximately $198 \times 10^6 B\bar{B}$ pairs.

The signal yields, N_{meas}, were obtained by employing simultaneous binned maximum-likelihood template fits to the p_e^B and p_μ^B spectra. The momentum range, $p_l^B\ \epsilon\ [1.3, 2.3]\ GeV/c$, was divided into 10 equal intervals (bins). The last bin includes any overflow events. The selection of the lower limit on p_l^B is motivated by the objective of minimizing background effects and effectively suppressing $B \to X\tau\nu$ decays to a negligible extent. The overall signal efficiencies are found by extracting the selected signal yields, denoted as N_{sel}^l, from fits to the simulated spectra. These yields are then divided by the number of generated events in the complete phase space, denoted as N_{gen}^l. The electron and muon efficiencies are obtained as $(1.62 \pm 0.03) \times 10^{-3}$ and $(2.04 \pm 0.05) \times 10^{-3}$, respectively.

The experimental p_l^B spectra are fitted in the same-charge control and opposite-charge signal samples, as shown in Figure 10. The fits yield $N_{meas}^e = 48030 \pm 290$ and $N_{meas}^\mu = 58,570 \pm 430$ signal events in the electron and muon modes, respectively.

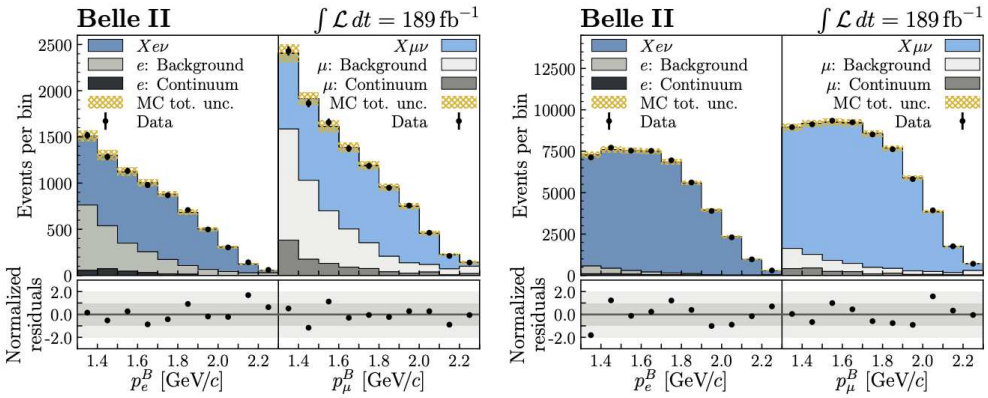

Figure 10. Same-charge control channel (**left**) and opposite-charge signal (**right**) spectra of the lepton momentum in the B_{sig} rest frame, p_l^B, with the fit results overlaid [42]. Hatched area shows the total statistical plus systematic uncertainty, added in quadrature in each bin.

Using the yields and efficiencies, the ratio is obtained using the following equation: $R(X_{e/\mu}) = (N^e_{meas}/N^\mu_{meas}) \cdot (N^\mu_{sel}/N^e_{sel}) \cdot (N^e_{gen}/N^\mu_{gen})$. The value obtained after adding the systematic uncertainties was $R(X_{e/\mu}) = 1.033 \pm 0.010 \pm 0.019$. This is the most accurate branching fraction test of the universality of decay to electrons and muons in semileptonic B decays. The measurement of the full phase space agrees with what the SM predicted.

The measurement in the full phase space is consistent with the SM prediction.

3.4. $B_s \to \phi\mu\mu$ Analysis

The transitions involving a b quark transforming into an s quark and producing a pair of oppositely charged leptons are not allowed to occur directly in the SM at the tree level. Instead, these transitions can only take place through higher-order electroweak (loop) diagrams. The aforementioned transitions serve as effective tools for investigating potential contributions from NP that extend beyond the SM. These contributions may manifest in competing diagrams and have a notable impact on the branching fractions and angular distributions of $b \to sl^+l^-$ decays. The angular distributions of the $B_s \to \phi\mu\mu$ decay were examined by an angular analysis, utilizing proton–proton (pp) collision data amounting to 3 fb^{-1} [43] that were collected by the LHCb experiment between 2011 and 2012. The results of this analysis indicated that the observed angular distributions were consistent with the predictions made by the SM. LHCb updated this result using a total integrated luminosity of $8.4 fb^{-1}$ [44], which corresponds to the data that were obtained at center-of-mass energies of 7 TeV in 2011, 8 TeV in 2012, and 13 TeV from 2016 to 2018, corresponding to the LHC Run 1 and Run 2 periods, respectively.

The differential decay rate equation of $B_s \to \phi(K^+k^-)\mu\mu$ decay rate depends on the dimuon invariant mass squared, q^2, three decay angles, θ_l, θ_K, and ϕ, and the decay time of the B_s^0 meson. The angle θ_l (θ_K) represents the angular deviation of the μ^- (K^-) particle relative to the trajectory of the B_s^0 meson in the center-of-mass frame of the $\mu^+\mu^-$ (K^+K^-) system. Additionally, ϕ denotes the angle between the planes formed by the $\mu^+\mu^-$ and K^+K^- particles in the center-of-mass frame of the B_s^0 meson.

For a particular q^2 region, the untagged CP-averaged angular decay rate equation for the $B_s \to \phi(K^+k^-)\mu\mu$ decay is obtained by measuring and integrating it throughout the B_s^0 decay time.

$$\frac{1}{d\Gamma/dq^2}\frac{d^3\Gamma}{dcos\theta_l dcos\theta_K d\phi} = \frac{9}{32\pi}[\tfrac{3}{4}(1-F_L)\cdot sin^2\theta_K + F_L\cdot cos^2\theta_K + \tfrac{1}{4}(1-F_L)$$
$$\cdot sin^2\theta_K\cdot cos2\theta_l - F_L cos^2\theta_K\cdot cos2\theta_l + S_3(sin^2\theta_K\cdot sin^2\theta_l\cdot cos2\Phi)+$$
$$S_4(sin2\theta_K\cdot sin2\theta_l\cdot cos\Phi) + A_5(sin2\theta_K\cdot sin\theta_l\cdot cos\Phi) + A_6 sin2\theta_K\cdot cos\theta_l +$$
$$S_7(sin2\theta_K\cdot sin\theta_l.sin\Phi) + A_8(sin2\theta_K\cdot sin2\theta_l\cdot sin\Phi)+$$
$$A_9(sin2\theta_K\cdot sin^2\theta_l\cdot sin2\Phi)],$$

where the angular observables F_L and S_3, S_4, and S_7 are the charge-conjugation parity (CP) averages, and A_{CP} and A_5, A_8, and A_9 are CP asymmetries. The T-odd CP asymmetries A_8 and A_9, which exhibit time-reversal-odd behavior, are of significant importance. In the SM, these asymmetries are expected to be around zero. However, in the presence of contributions from new physics (NP), they can attain substantial magnitudes. The analysis conducted in this paper is unable to access the CP-averaged observable S_5 ($P_5^{'}$) due to the unknown decay flavor of the B_s^0 meson. This observable has been extensively studied in the context of $B^0 \to K^{*0}\mu^+\mu^-$ decays.

The determination of angular observables entails employing an UML fit to the mass distribution of the invariant $K^+K^-\mu^+\mu^-$, in addition to the three decay angles: θ_l, θ_K, and ϕ. The fitting technique is performed by dividing the q^2 region below 12.5 GeV^2/c^4 into separate thin sections, each with a width of approximately 2 GeV^2/c^4. The angular observables are shown in Figure 11, overlaid with SM predictions. There are no predictions for S_7 or A_5,A_6, A_8, or A_9 as they are expected to be close to zero in the SM.

The measurement of the branching fraction of $B_s \to \phi\mu\mu$ [44,45] in $q^2\epsilon[1.1, 6.0]$ region by the LHCb collaboration has discrepancy at the level of 3.6 σ (Figure 12) from the SM expectations [28,29].

Several SM predictions have been published recently for $B_s \to \phi\mu\mu$, $B_s \to f_2^{'}\mu\mu$ and $\Lambda_b \to \Lambda(\to p\pi^-)l^+l^-$ decays [46,47].

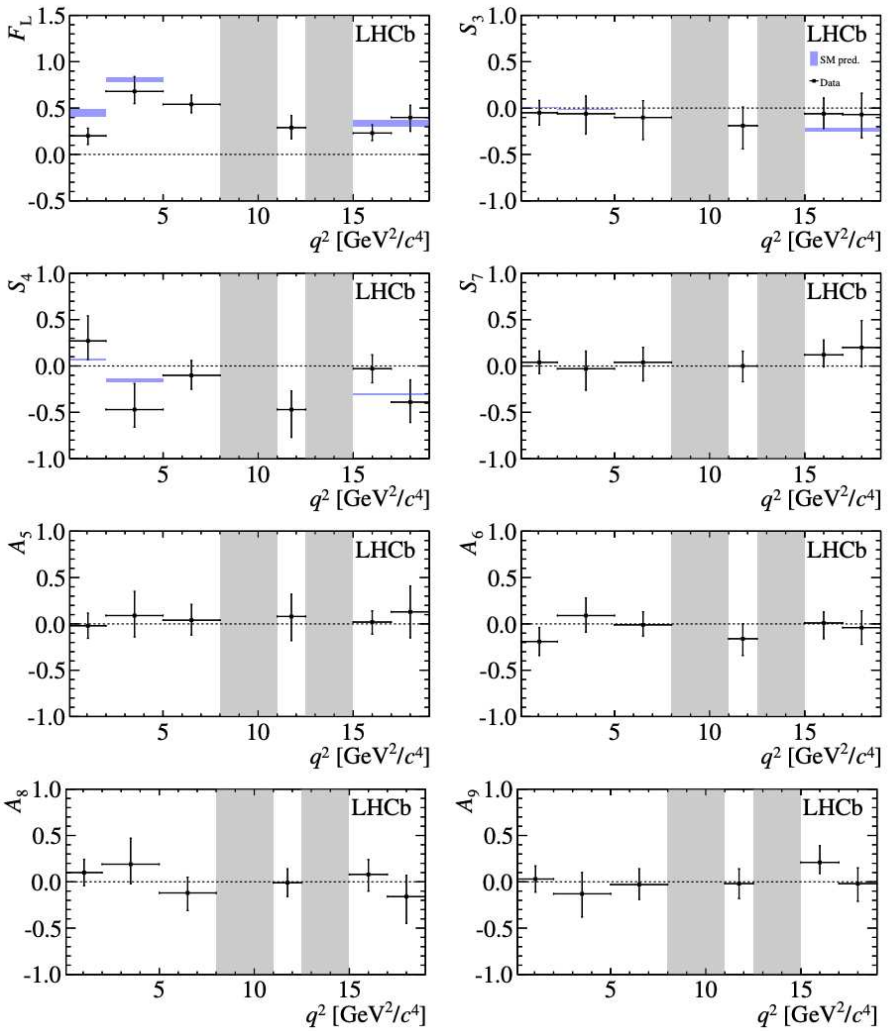

Figure 11. CP-averaged angular observables F_L and S_3, S_4, and S_7, and CP asymmetries A_5, A_6, A_{58}, and A_9 [43], shown by black dots overlaid with SM predictions, where available, indicated as blue shaded boxes. The gray areas are the charmonium resonance regions that are vetoed.

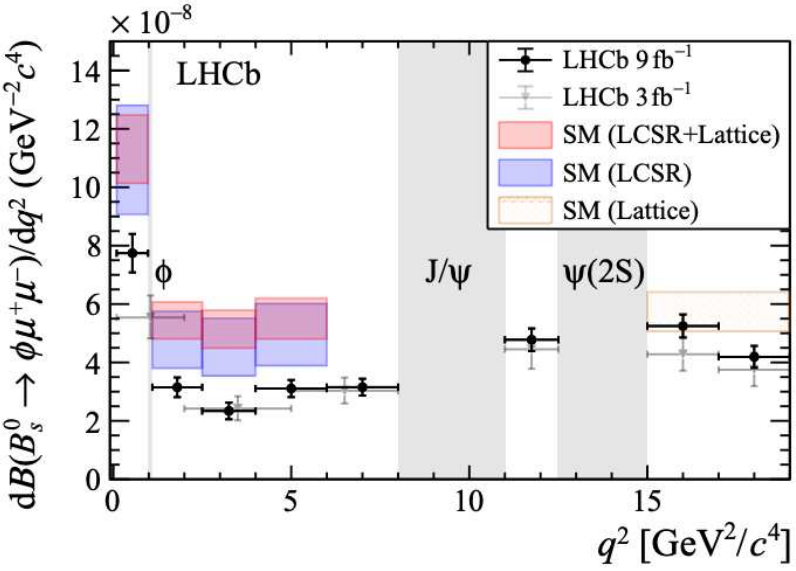

Figure 12. Differential branching fraction $dB(B_s^0 \to \phi\mu^+\mu^-/dq^2)$ overlaid with SM predictions [44] using light cone sum rules at low q^2 and Lattice calculations at high q^2. Previous LHCb results using 3 fb^{-1} are shown with gray markers.

3.5. Lepton Universality in Charged-Current Transitions $b \to clv$: R_D, R_{D^*} Analyses

The $b \to c$ tree-level transitions offer a unique set of decays to study lepton flavor universality. The rates of b-meson decays to τ and μ leptons are expected to differ because of the substantial mass difference between τ and μ leptons. The ratio of the exclusive decays with τ lepton can be defined as:

$$R_D^{(*)} = \frac{\Gamma(B \to D^{(*)}\tau\bar{\nu_\tau})}{\Gamma(B \to D^{(*)}l\bar{\nu_l})}$$

This is a very clean final state experimentally due to the fact that the entire decay chain can be fully reconstructed. Combined results by Belle [48–50], BaBar [51,52], and the LHCb [53,54] collaboration yield a tension of 3.8 σ with the SM. However, this tension has decreased to 3.1 σ with the recent Belle measurement [55].

LHCb collaboration had announced the first simultaneous measurements of the ratio of the branching fraction of B-meson decays to D mesons: $R(D^*) = \frac{BR(B\to D^*\tau^-\bar{\nu_\tau})}{BR(B\to D^*\mu^-\bar{\nu_\mu})}$, and $R(D) = \frac{BR(B\to D^0\tau^-\bar{\nu_\tau})}{BR(B\to D^0\mu^-\bar{\nu_\mu})}$ at a hadron collider.

Using only Run 1 data recorded at a center-of-mass energy of 7 and 8 TeV, LHCb collaboration observed $R(D^*) = 0.281 \pm 0.018(stat.) \pm 0.024(syst.)$ and $R(D) = 0.441 \pm 0.060(stat.) \pm 0.066(syst.)$. The values are consistent with the SM prediction [40,56] within 1.9 σ. Figures 13 and 14 show the current status of these observables $R(D^{(*)})$, as reported by various experiments [31].

The τ polarization fraction and the longitudinal polarization fraction of D^* meson in $B \to D^*\tau\nu$ and $B \to J/\psi\tau\nu$ have $(1.4\sigma)2.5\,\sigma$ [48,49] and 1.8 σ [50] deviations, respectively.

Both $R(K)$ and $R(D(*))$ measurements are crucial tests for LFU. The global fits of $R(D(*))$ measurements show that the ratio of B-meson to D-meson decays tends to be larger (by about 3.2 σ) than the SM prediction.

Since τ lepton is much heavier than the μ lepton, it is expected to observe differences in the rates of b-meson decays.

$$R_D^{(*)} = \frac{\Gamma(B \to D^{(*)}\tau\bar{\nu_\tau})}{\Gamma(B \to D^{(*)}l\bar{\nu_l})}$$

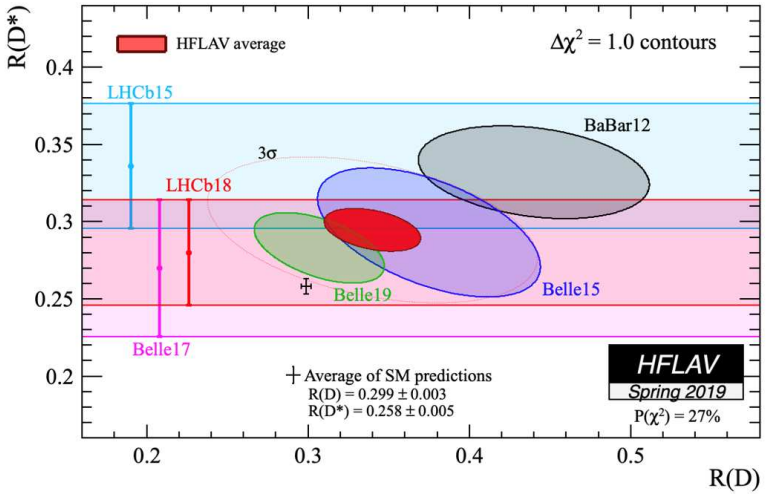

Figure 13. Plot showing $R(D)$ and $R(D^*)$ values obtained by the BaBar, Belle, and LHCb collaborations by the heavy flavor averaging group [57].

The predictions for the ratios $R(D)$ and $R(D^*)$ in the Standard Model (SM) exhibit a high level of accuracy due to their independence from errors arising from the CKM-matrix element V_{cb} and hadronic matrix elements. The revised values of $R(D)$ and $R(D^*)$ align with both the current world average compiled by the HFLAV collaboration [57] and the SM prediction, with a significance of at 2.2 σ and 2.3 σ, respectively. The collective outcome of the LHCb experiment yields enhanced sensitivity in detecting potential deviations from lepton universality.

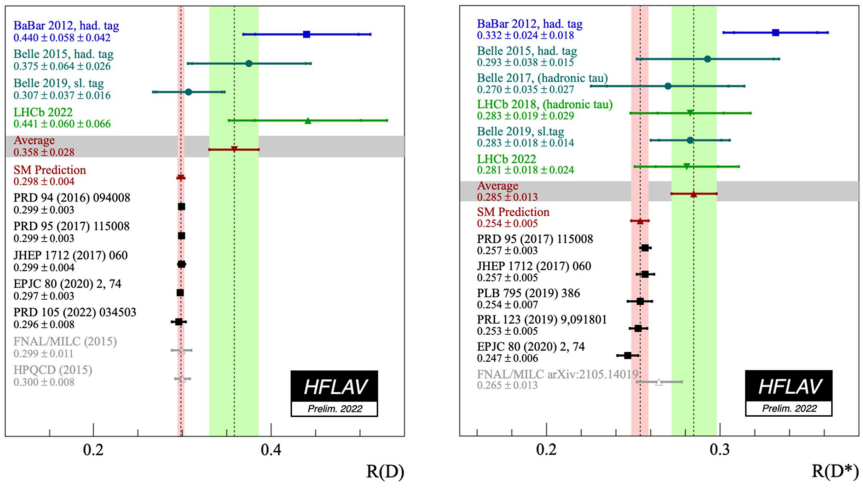

Figure 14. Lepton universality results (left) R(D) and (right) $R(D^*)$ obtained by the BaBar, Belle, and LHCb collaborations [57].

3.6. R_Ω Measurement

LFU in Ω_c^0 is probed for the first time $\Omega_c^0 \to \Omega^0 l^+ \nu_l$ decays using 89.5, 711, and 121.1 fb^{-1} data collected at the center-of-mass energies of 10.52, 10.58, and 10.86 GeV at Belle [58]. Signal yields are extracted by binned ML fits to the invariant mass spectra. The significance of the $\Omega_c^0 \to \Omega^0 l^+ \nu_l$ is larger than 10 σ, and $\Omega_c^0 \to \Omega^0 \mu^+ \nu_\mu$ decay is observed for the first time in Belle. The obtained signal yields are 865.3 ± 35.3, 707.6 ± 37.7, and 367.9 ± 31.4 signal events for $\Omega_c^0 \to \Omega^0 \pi^+$, $\Omega_c^0 \to \Omega^- e^+ \nu_l$, and $\Omega_c^0 \to \Omega^- \mu^+ \nu_\mu$, respectively (Figure 15). The ratio of the branching fractions of $\Omega_c^0 \to \Omega^- e^+ \nu_l$ and $\Omega_c^0 \to \Omega^- \mu^+ \nu_\mu$, $R(\Omega)$ was obtained as $1.02 \pm 0.10 \pm 0.02$ [59], which is consistent with the expectation of lepton flavor universality, 1.03 ± 0.06 [57]. This is the first test of LFU in the charmed baryon decays using data of the Belle experiment.

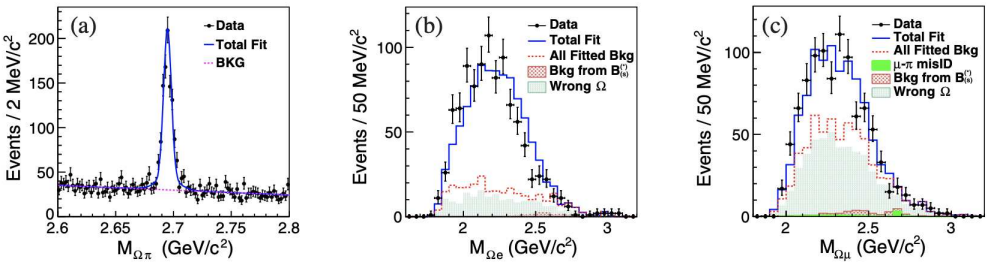

Figure 15. The fits to the (**a**) $M_{\Omega\pi}$, (**b**) $M_{\Omega e}$, and (**c**) $M_{\Omega\mu}$ distributions for the selected candidates from data [59]. Dots with error bars represent the data, solid lines are the best fits, and dashed lines are the fitted total backgrounds.

4. Conclusions

Recent research has shown that studying flavor anomalies in high-energy physics is a popular and active topic. The reasoning behind this phenomenon might be attributed to the recognition of signs that imply possible inconsistencies between the experimental results and the predictions generated from the Standard Model. The most recent observations of branching fractions and angular distributions in the decays of $b \to s\mu^-\mu^+$ have predominantly relied on accurate data from the Large Hadron Collider beauty (LHCb) experiment. These measurements have revealed a notable and constant deviation from the predicted outcomes, according to the SM. Tensions have been identified in the LFU tests conducted on R_K, R_{K^*}, and R_{pK} as well. While the individual data exhibit tensions with varied significance levels ranging from 2 to 3 σ, the amalgamation of these measurements yields a coherent depiction. Formulating a definitive conclusion about the LFU presents a considerable challenge. There is potential for further developments in the investigation of "flavour anomalies" with the collection of additional data by LHCb, CMS, and Belle II. These experiments aim to identify any potential violations of LFU.

Though the very recent measurements of R_K and R_K^* are consistent with the SM, the excitement remains on the measurements of the LHCb experiment with the observables $B(B_s \to \phi\mu^+\mu^-)$, which have deviations at the level of 3.6 σ. Additionally, standard deviations of 3.3 σ and 1.2 σ, respectively, for P_5' in $B \to K^*\mu^+\mu^-$ and the branching ratio in $B_s \to \mu^+\mu^-$ processes are observed.

The charged current transitions conducted by the B-factory experiments, Babar and Belle, as well as by LHCb, have yielded indications of lepton-flavor violating searches. These findings suggest the possibility of lepton-flavor universality breaking in tree-level $b \to cl\nu_l$ transitions. The major measurements in this sector involve the lepton flavor universality ratios R_D, R_{D^*} and $R_{J/\psi}$, which pertain to the tauonic and muonic decays. The average of the individual R_D and R_{D^*} measurements obtained from the experiment exhibits a significant discrepancy, with a tension of more than 3 σ significance, when compared to the prediction made by the SM.

Two further intriguing $b \to sll$ processes include the decays $B_s \to \phi\mu\mu$ and $B_s \to f_2'\mu\mu$. The Large Hadron Collider beauty (LHCb) experiment has yielded the most accurate results to date regarding the decay process of $b \to s\mu^+\mu^-$. Nevertheless, it is worth noting that a significant portion of the analyses conducted thus far have not fully utilized the complete dataset from LHC Run 1 and 2. Consequently, we can anticipate a multitude of intriguing experimental findings in the coming times. The inclusion of data sample from Run 3 will enhance the accuracy of the findings. Other LHC experiments like ATLAS and CMS will also play a major role.

In addition to the experiments conducted at the Large Hadron Collider (LHC), the Belle II experiment will also contribute to the field by offering more precise measurements of inclusive decays. Consequently, it will serve as a crucial component in independently confirming the findings obtained from the LHC experiments.

Although the Standard Model (SM) has achieved remarkable success as a mathematical framework, it still does not account for several mysteries. This work examines the current state of LFU violation anomalies in B physics, considering both theoretical and experimental perspectives. These anomalies have the potential to provide new insights into the gathering and analysis of data, hence offering explanations far beyond the Standard Model (BSM) physics. In recent times, the LFU ratios associated with neutral-current (R_K, R_{K^*}) have been discovered to align with the predictions of the SM and are considered to be observables that possess theoretical integrity. The recently revised results for (R_D, R_{D^*}) have been presented, demonstrating a significant overall significance within a range of 3 σ. There are new results expected for the $b \to sll$ channels, which could shed more light on the flavor anomalies. In conclusion, the outlook for the future appears highly favorable, as forthcoming findings are anticipated from the collaborative efforts of CMS, LHCb, and Belle II. The future has promising prospects for both theorists and experimentalists.

Funding: This research received no external funding.

Data Availability Statement: No new data were created or analyzed in this study. Data sharing is not applicable to this article.

Acknowledgments: The author would like to acknowledge the support rendered by her institute, Indian Institute of Technology Bhubaneswar, India.

Conflicts of Interest: The author declares no conflict of interest.

Abbreviations

The following abbreviations are used in this manuscript:

SM	Standard Model
LFU	Lepton flavor universality
NP	New physics
BSM	Beyond Standard Model
GIM	Glashow, Illiopoulos, and Maiani
QCD	Quantum chromodynamics
LHC	Large Hadron Collider
EFT	Effective field theories
OPE	Operator product expansion
CKM	Cabibbo–Kobayashi–Maskawa
UML	Unbinned maximum likelihood
LQCD	Lattice quantum chromodynamics
PDF	Probability density function
CP	Charge-conjugation parity
LHCb	Large Hadron Collider beauty
CMS	Compact Muon Solenoid
ATLAS	A Toroidal LHC Apparatus

References

1. Ali, A.; Giudice, G.F.; Mannel, T. Towards a Model-Independent Analysis of Rare B Decays. *Z. Phys. C* **1995**, *67*, 417–432. [CrossRef]
2. Cabibbo, N. Unitary Symmetry and Leptonic Decays. *Phys. Rev. Lett.* **1963**, *10*, 531–533. [CrossRef]
3. Aubert, B; Barate, R.; Boutigny, D.; Couderc, F.; del Amo Sanchez, P.; Gaillard, J.-M.; Hicheur, A.; Karyotakis, Y.; Lees, J.P.; Poireau, V.; et al. The BABAR Detector: Upgrades, Operation and Performance. *Nucl. Instrum. Methods A* **2013**, *729*, 615–701. [CrossRef]
4. Abashian, A.; Gotow, K.; Morgan, N.; Piilone, L.; Schrenk, S.; Abe, K.; Adachi, I.; Alexander, J.P.; Aoki, K.; Behari, S.; et al. The Belle detector. *Nucl. Instrum. Methods A* **2002**, *479*, 117–232. [CrossRef]
5. Acosta, D.; Adelman, J.; Affolder, T.; Akimoto, T.; Albrow, M.G.; Ambrose, D.; Amerio, S.; Amidei, D.; Anastassov, A.; Anikeev, K.; et al. Measurement of the J/Ψ Meson and b-Hadron Production Cross Sections in ppbar Collisions at $\sqrt{s}$ = 1960 GeV. *Phys. Rev. D* **2005**, *71*, 032001. [CrossRef]
6. Abazov, V.M.; Abbott, B.; Abolins, M.; Acharya, B.S.; Adams, D.L.; Adams, M.; Adams, T.; Agelou, M.;Agram, J.-L.; Ahmed, S.N.; et al. The Upgraded D0 Detector. *Nucl. Instrum. Methods A* **2006**, *565*, 463–537. [CrossRef]

7. The ATLAS Collaboration; Aad, G.; Abat, E.; Abdallah, A; Abdelalim, A.A.; Abdesselam, A.; Abdinov, O.; Abi, B.A.; Abolins, M.; Abramowicz, H.; et al. The ATLAS Experiment at the CERN Large Hadron Collider. *J. Instrum.* **2008**, *3*, S08003. [CrossRef]
8. The CMS Collaboration; Chatrchyan, S.; Hmayakyan, G.; Khachatryan, V.; Sirunyan, A.M.; Adam, W.; Bauee, T.; Bergauer, T.; Bergauer, H.; Dragicevic, N.; et al. The CMS experiment at the CERN LHC. *J. Instrum.* **2008**, *3*, S08004. [CrossRef]
9. The LHCb Collaboration; Augusto Alves, A. Jr.; Andrade Filho, L.M.; Barbosa, A.F.; Bediaga, I.; Cernicchiaro, G.; Guerrer, G.; Lima, H.P., Jr.; Machado, A.A.; Magnin, J.; et al. The LHCb Detector at the LHC. *J. Instrum.* **2008**, *3*, S08005. [CrossRef]
10. Wilson, K.G.; Zimmermann, W. Operator product expansions and composite field operators in the general framework of quantum field theory. *Comm. Math. Phys.* **1972**, *24*, 87–106. [CrossRef]
11. Kobayashi, M.; Maskawa T. CP-Violation in the Renormalizable Theory of Weak Interaction. *Prog. Theor. Phys.* **1973**, *49*, 652–657. [CrossRef]
12. Aaboud, M. Angular analysis of $B_d^0 \to K^* \mu^+ \mu^-$ decays in pp collisions at $\sqrt{s} = 8$ *TeV* with the ATLAS detector. *J. High Energy Phys.* **2018**, *10*, 047.
13. Sirunyan, A.M. Measurement of angular parameters from the decay $B^0 \to K^{*0} \mu^+ \mu^-$ in proton-proton collisions at $\sqrt{}$ = 8 TeV. *Phys. Lett. B* **2018**, *781*, 517–541. [CrossRef]
14. Wehle, S. Angular analysis of $B^0 \to K^{*0}(892) l^+ l^-$. In Proceedings of LHCSki2016: A First Discussion of 13 TeV Results, Obergurgl, Austria, 10–15 April 2016.
15. Choudhury, S.; Sandilya, S.; Trabelsi, K.; Giri, A.; Aihara, H.; Al Said, S.; Asner, D.M.; Atmacan, H.; Aulchenko, V.; Aushev, T.; et al. Test of lepton flavor universality and search for lepton flavor violation in $B \to Kll$ decays. *arXiv* **2022**, arXiv:1908.01848.
16. Belle Collaboration; Wehle, S.; Niebuhr, C.; Yashchenko, S.; Adachi, I.; Aihara, H.; Al Said, S.; Asner, D.M.; Aulchenko, V.; Aushev, T.; et al. Lepton-flavor-dependent angular analysis of $B \to K^* ll$. *Phys. Rev. Lett.* **2017**, *118*, 111801. [CrossRef]
17. Belle Collaboration; Wehle, S.; Adachi, I.; Adamczyk, K.; Aihara, H.; Asner, D.M.; Atmacan, H.; Aulchenko, V.; Aushev, T.; Ayad, R.; et al. Test of lepton-flavor universality in $B \to K^* ll$ decays at Belle. *Phys. Rev. Lett.* **2021**, *126*, 181801. [CrossRef]
18. BaBar Collaboration; Lees, J.P. Measurement of branching fractions and rate asymmetries in the rare $B \to K^{(*)} ll$ decays. *Phys. Rev. D* **2012**, *86*, 032012. [CrossRef]
19. LHCb Collaboration; Aaij, R.; Adeva, B.; Adinolfi, M.; Ajaltouni, Z.; Akar, S.; Albrecht, J.; Alessio, F.; Alexander, M.; Ali, S.; et al. Test of lepton universality using $B^+ \to K^+ ll$ decays. *Phys. Rev. Lett.* **2014**, *113*, 151601. [CrossRef]
20. LHCb Collaboration; Aaij, R.; Adeva, B.; Adinolfi, M.; Ajaltouni, Z.; Akar, S.; Albrecht, J.; Alessio, F.; Alexander, M.; Ali, S.; et al. Test of lepton universality with $B^0 \to K^{*0} ll$ decays. *J. High Energy Phys.* **2017**, *8*, 055. [CrossRef]
21. LHCb Collaboration; Aaij, R.; Abellán Beteta, C.; Adeva, B.; Adinolfi, M.; Aidala, C.A.; Ajaltouni, Z.; Akar, S.; Albicocco, P.; Albrecht, J.; et al. Search for lepton-universality violation in $B^+ \to K^+ l^+ l^-$decays. *Phys. Rev. Lett.* **2019**, *122*, 191801. [CrossRef]
22. LHCb Collaboration; Aaij, R.; Abellán Beteta, C.; Ackernley, T.; Adeva, B.; Adinolfi, M.; Afsharnia, H.; Aidala, C.A.; Aiola, S.; Ajaltouni, Z.; et al. Test of lepton universality using $\Lambda_b^0 \to pK^- l^+ l^-$ decays. *J. High Energy Phys.* **2020**. [CrossRef]
23. LHCb Collaboration; Aaij, R. Test of lepton universality in beauty-quark decays. *Nat. Phys.* **2022**, *18*, 277.
24. LHCb Collaboration; Aaij, R.; Abdelmotteleb, A.S.W.; Abellán Beteta, C.; Abudinén, F.; Ackernley, T.; Adeva, B.; Adinolfi, M.; Afsharnia, H.; Agapopoulou, C.; et al. Tests of lepton universality using $B^0 \to K_s^0 ll$ and $B^+ \to K^{*+} ll$ decays. *Phys. Rev. Lett.* **2022**, *128*, 191802. [CrossRef] [PubMed]
25. Aaij, R.; LHCb Collaboration. Measurement of CP-Averaged Observables in the $B^0 \to K^{*0}(892) \mu^+ \mu^-$ Decay. *Phys. Rev. Lett.* **2020**, *125*, 011802. [CrossRef]
26. Aaij, R.; Adeva, B.; Adinolfi, M. Measurement of Form-Factor-Independent Observables in the Decay $B^0 \to K^{*0} \mu^+ \mu^-$. *Phys. Rev. Lett.* **2013**, *111*, 191801. [CrossRef]
27. Aaij, R. Angular analysis of the $B^0 \to K^{*0} \mu^+ \mu^-$ decay using 3 fb^{-1} of integrated luminosity. *J. High Energy Phys.* **2016**, *2*, 104. [CrossRef]
28. Aebischer, J.; Kumar, J.; Stangl, P.; Straub, D.M. A Global Likelihood for Precision Constraints and Flavour Anomalies. *Eur. Phys. J. C* **2019**, *79*, 509. [CrossRef]
29. Bharucha, A.; Straub, D.M.; Zwicky, R. $B \to Vll$ in the Standard Model from light-cone sum rules. *J. High Energy Phys.* **2016**, *8*, 098. [CrossRef]
30. Aaij, R.; Abdelmotteleb, A.S.W.; Abellan Beteta, C.; Abudinén, F.; Ackernley, T.; Adeva, B.; Adinolfi, M.; Adlarson, P.; Afsharnia, H.; Agapopoulou, C.; et al. Test of lepton universality in $b \to sl^+ l^-$ decays. *arXiv* **2022**, arXiv:2212.09152.
31. Aaij, R.; Abdelmotteleb, A.S.W.; Abellan Beteta, C.; Abudinén, F.; Ackernley, T.; Adeva, B.; Adinolfi, M.; Adlarson, P.; Afsharnia, H.; Agapopoulou, C.; et al. Measurement of lepton universality parameters in $B^+ \to K^+ l^+ l^-$ and $B^0 \to K^{*0} l^+ l^-$ decays. *arXiv* **2022**, arXiv: 2212.09153.
32. Belle II Collaboration; Abudinén, F.; Adachi, I.; Adak, R.; Adamczyk, K.; Aggarwal, L.; Ahlburg, P.; Ahmed, H.; Ahn, J.K.; Aihara, H.; et al. Measurement of the branching fraction for the decay B → K*(892)$\ell^+ \ell^-$ at Belle II. *arXiv* **2022**, arXiv: 2206.05946.
33. Flavour Lattice Averaging Group Collaboration. FLAG Review 2019. *arXiv* **2019**, arXiv:1902.08191.
34. Hughes, C.; Davies, C.T.H.; Monahan, C.J. New methods for B meson decay constants and form factors from lattice NRQCD. *Phys. Rev. D* **2018**, *97*, 054509. [CrossRef]
35. Bobeth, C.; Gorbahn, M.; Stamou, E. Electroweak corrections to $B_{s,d} \to l^+ l^-$. *Phys. Rev. D* **2014**, *89*, 034023. [CrossRef]
36. Hermann, T.; Misiak, M.; Steinhauser, M. Three-loop QCD corrections to $B_s \to \mu^+ \mu^-$. *J. High Energy Phys.* **2013**, *12*, 097. [CrossRef]

37. CMS Collaboration; Sirunyan, A.M.; Tumasyan, A.; Adam, W.; Ambrogi, F.; Bergauer, T.; Brandstetter, J.; Dragicevic, M.; Erö, J.; Escalante Del Valle, A. Measurement of properties of $B_s \to \mu^+\mu^-$ decays and search for $B_0 \to \mu^+\mu^-$ with the CMS experiment. *J. High Energy Phys.* **2020**, *4*, 188. [CrossRef]
38. Pivk, M.; Le Diberder, F.R. SPlot: A statistical tool to unfold data distributions. *Nucl. Instrum. Meth. A* **2005**, *555*, 356–369. [CrossRef]
39. LHCb Collaboration; Aaij, R.; Beteta, C.A.; Ackernley, T.; Adeva, B.; Adinolfi, M.; Afsharnia, H.; Aidala, C.A.; Aiola, S.; Ajaltouni, Z.; et al. Measurement of the $B_s^0 \to \mu^+\mu^-$branching fraction and effective lifetime and search for $B^0 \to \mu^+\mu^-$ decays. *Phys. Rev. Lett.* **2017**, *118*, 191801. [CrossRef]
40. Bigi, D.; Gambino, P.; Schacht, S. $R(D^*)$, $|V_{cb}|$, and the Heavy Quark Symmetry relations between form factors. *J. High Energy Phys.* **2017**, *11*, 1–23. [CrossRef]
41. Tumasyan, A.; Adam, W.; Andrejkovic, J.W.; Bergauer, T.; Chatterjee, S.; Damanakis, K.; Dragicevic, M.; Escalante Del Valle, A.; Hussain, P.S.; Jeitler, M.; et al. Measurement of $B_s^0 \to \mu^+\mu^-$ decay properties and search for the $B^0 \to \mu^+\mu^-$ decay in proton-proton collisions at $\sqrt{s}$ = 13 TeV. *Phys. Lett. B* **2023**, *842*, 137955. [CrossRef]
42. Aggarwal, L.; Ahmed, H.; Aihara, H.; Akopov, N.; Aloisio, A.; Anh Ky, N.; Asner, D.M.; Atmacan, H.; Aushev, T.; Aushev, V.; et al. A test of light-lepton universality in the rates of inclusive semileptonic B-meson decays at Belle II. *arXiv*, **2022**, arXiv:2301.08266.
43. Aaij, R.; Abellan Beteta, C.; Adeva, B.; Adinolfi, M.; Adrover, C.; Affolder, A.; Ajaltouni, Z.; Albrecht, J.; Alessio, F.; Alexander, M.; et al. Differential branching fraction and angular analysis of the $B_s^0 \to \phi\mu^+\mu^-$ decay. *J. High Energy Phys.* **2013**, *7*, 1308.
44. Aaij, R.; Adeva, B.; Adinolfi, M.; Affolder, A.; Ajaltouni, Z.; Akar, S.; Albrecht, J.; Alessio, F.; Alexander, M.; Ali, S.; et al. Angular analysis and differential branching fraction of the $B_s^0 \to \phi\mu^+\mu^-$ decay. *J. High Energy Phys.* **2015**, *9*, 179. [CrossRef]
45. Aaij, R.; Abellán Beteta, C.; Ackernley, T.; Adeva, B.; Adinolfi, M.; Afsharnia, H.; Aidala, C.A.; Aiola, S.; Ajaltouni, Z.; et al. Branching Fraction Measurements of the Rare $B_s^0 \to \phi\mu^+\mu^-$ and $B_s^0 \to f_2'\mu^+\mu^-$ Decays, *Phys. Rev. Lett.* **2021**, *127*, 151801. [CrossRef]
46. Rajeev, N.; Sahoo, N.; Dutta, R. Angular analysis of $B_s \to f_2'(1525)(\to K^+K^-)\mu^+\mu^-$ decays as a probe to lepton flavor universality violation, *Phys. Rev. D 103*, 095007. [CrossRef]
47. Das, D.; Das, J.; Kumar, G.; Sahoo, N. $\Lambda_b \to \Lambda(\to p\pi^-)l^+l^-$ as probe of CP-violating New Physics. *arXiv*, **2022**, arXiv:2211.09065.
48. Hirose, S.; Iijima, T.; Adachi, I.; Adamczyk, K.; Aihara, H.; Al Said, S.; Asner, D.M.; Atmacan, H.; Aushev, T.; Ayad, R.; et al. Measurement of the τ lepton polarization and $R(D^*)$ in the $\bar{B} \to D^*\tau^-\bar{\nu_\tau}$ decay. *Phys. Rev. Lett.* **2017**, *118*, 211801. [CrossRef]
49. Hirose, S.; Iijima, T.; Adachi, I.; Adamczyk, K.; Aihara, H.; Al Said, S.; Asner, D.M.; Atmacan, H.; Aushev, T.; Ayad, R.; et al. Measurement of the lepton polarization and $R(D^*)$ in the $\bar{B} \to D^*\tau^-\bar{\nu_\tau}$ decay with one-prong hadronic decays at Belle. *Phys. Rev. D* **2018**, *97*, 012004. [CrossRef]
50. Abdesselam, A.; Adachi, I.; Adamczyk, K.; Ahn, J. K.; Aihara,H.; Al Said, S.; Arinstein, K.; Arita, Y.; Asner, D.M.; Atmacan, H.; et al. Measurement of the D^{*-} polarization in the $B^0 \to D^{*-}\tau^+\nu_{tau}$ decay. In Proceedings of the 10th International Workshop on the CKM Unitarity Triangle, Mumbai, India, 28 November–10 December 2019.
51. Lees, J.P.; Poireau, V.; Tisserand, V.; Garra Tico, J.; Grauges, E.; Palano, A.; Eigen, G.; Stugu, B.; Brown, D.N.; Kerth, L.T.; et al. Evidence for an excess of $B \to D^{(*)}\tau\nu$ Decays. *Phys. Rev. Lett.* **2012**, *109*, 101802. [CrossRef]
52. Lees, J.P.; Poireau, V.; Tisserand, V.; Grauges, E.; Palano, A.; Eigen, G.; Stugu, B.; Brown, D.N.; Kerth, L.T.; Kolomensky, Y.G.; et al. Measurement of an Excess of $B \to D^{(*)}\tau\nu$ Decays and Implications for Charged Higgs Bosons. *Phys. Rev. D* **2013**, *88*, 072012. [CrossRef]
53. Aaij, R. LHCb. *Phys. Rev. Lett.* **2015**, *115*, 111803; Erratum: *Phys. Rev. Lett.* **2015**. *115*, 159901. [CrossRef]
54. Aaij, R.; Adeva, B.; Adinolfi, M.; Ajaltouni, Z.; Akar, S.; Albrecht, J.; Alessio, F.; Alexander, M.; Alfonso Albero, A.; Ali, S.; et al. Measurement of the ratio of the $B^0 \to D^{*-}\tau^+\nu_\tau$ and $B^0 \to D^{*-}\mu^+\nu_\mu$ branching fractions using three-prong τ-lepton decays. *Phys. Rev. Lett.* **120**, *171802*. [CrossRef] [PubMed]
55. Caria, G.; Urquijo, P.; Adachi, I.; Aihara, H.; Al Said, S.; Asner, D.M.; Atmacan, H.; Aushev, T.; Babu, V.; Badhrees, I.; et al. Measurement of $R(D)$ and $R(D^*)$ with a Semileptonic Tagging Method. *Phys. Rev. Lett.* **2020**, *124*, 161803. [CrossRef] [PubMed]
56. Jaiswal, S.; Nandi, S.; Patra, S.K. Updates on extraction of |Vcb| and SM prediction of $R(D^*)$ in $B \to D^*lv_l$ decays. *J. High Energy Phys.* **2020**, 165. [CrossRef]
57. Amhis, Y.; Banerjee, S.; Ben-Haim, E.; Bertholet, E.; Bernlochner, F.U.; Bona, M.; Bozek, A.; Bozzi, C.; Brodzicka, J.; Chobanova, V.; et al. Averages of b-hadron, c-hadron, and τ-lepton properties as of 2018. *Eur. Phys. J. C* (**2021**), *81*, 226. [CrossRef]
58. Huang, F.; Zhang, Q.-A. Angular Distributions for Multi-body Semileptonic Charmed Baryon Decays. *Eur. Phys. J. C* **2022**, *82*, 11. [CrossRef]
59. Li, Y.B.; Shen C.P.; Adachi, I.; Aihara, H.; Al Said, S.; Asner, D.M.; Atmacan, H.; Aushev, T.; Ayad, R.; Babu, V.; Bahinipati, S.; et al. First test of lepton flavor universality in the $\Omega_c^0 \to \Omega^0 l^+\nu_l$ charmed baryon decays using data of the Belle experiment. *Phys. Rev. D* **2022**, *105*, L091101. [CrossRef]